Available online at www.sciencedirect.com
ScienceDirect
Journal of Power Sources 169 (2007) 59–64
JOURNAL OF POWER SOURCES
www.elsevier.com/locate/jpowsour

Short communication

Platinum supported on functionalized ordered mesoporous carbon as electrocatalyst for direct methanol fuel cells☆

L. Calvillo[a], M.J. Lázaro[a,*], E. García-Bordejé[a], R. Moliner[a], P.L. Cabot[b], I. Esparbé[b], E. Pastor[c], J.J. Quintana[c]

[a] *Instituto de Carboquímica (CSIC), Miguel Luesma Castán 4, 50018 Zaragoza, Spain*
[b] *LEMMA, Departamento de Química Física, Universidad de Barcelona, Martí i Franquès 1-11, 08028 Barcelona, Spain*
[c] *Departamento de Química Física, Universidad de La Laguna, Avda. Astrofísico Francisco Sánchez s/n, 38071 La Laguna, Santa Cruz de Tenerife, Spain*

Available online 30 January 2007

Abstract

Ordered mesoporous carbon (OMC) with a specific area of 570 $m^2\ g^{-1}$ was synthesised using mesoporous silica SBA-15 as template. OMC was used as platinum catalyst support using the method of reduction with $NaBH_4$. Before deposition of platinum, the texture and surface chemistry of the support were modified by oxidation treatments in liquid phase using nitric acid as oxidative agent. During the oxidation process, oxygen surface groups were created, whereas ordered porous structure was maintained, as temperature programmed desorption and transmission electronic microscopy showed, respectively. Platinum supported materials were well dispersed over the mesoporous support and its catalytic performance towards methanol oxidation improved when compared with commercial carbon (Vulcan XC-72).

Keywords: Ordered mesoporous carbon; Electrocatalyst; DMFC; CO oxidation; Electrochemical characterization

1. Introduction

It is expected that the traditional systems for energy generation would be replaced by fuel cells in a medium long term. The most developed fuel cells are polymeric electrolyte fuel cells, PEMFC and DMFC, the latter using methanol directly as combustible. However, there are several aspects concerning its components that need to be improved. For this objective, the synthetic carbonaceous materials with controllable surface and functional properties can supply innovative solutions. Nowadays, the most commonly used electrocatalyst, both in cathode and anode, is platinum supported on carbon blacks [1–6]. However, it is necessary to obtain a more effective catalyst, both in catalytic performance and electric conductivity. To achieve a higher efficiency of the electrocatalysts, platinum has to be well dispersed on the support. For this reason, it is desirable that the support material provides a suitable specific area and surface chemistry as well as a good electrical conductivity.

Recently, novel non-conventional carbon materials have attracted much interest as electrocatalyst support because of their good electrical and mechanical properties. The examples are supports produced from carbon nanofibers [7–10], carbon nanotubes [11–13], carbon aerogels [14–17] or ordered mesoporous carbons (OMC) [18–21]. The electrocatalysts supported on these non-conventional carbon materials have a better performance in methanol electrooxidation than commercial ones. The ordered mesoporous carbons have received great attention because of their potential use as catalytic supports in fuel cell electrodes since the discovery of the mesoporous silica materials. They have controllable pore sizes, high surface areas and large pore volumes [22–24]. However, they contain a small amount of oxygen surface groups, which is disadvantageous for many applications. The relevance of the functionalization of carbon supports on the dispersion and anchoring of platinum particles on the support has been reported in the literature [25–28]. However, the functionalization of OMC has not been studied in a large extent because their ordered structure could collapse during the process. Ryoo et al. [29] reported in a previous study that ordered mesoporous carbons can maintain an ordered structure even in boiling 5 M aqueous solution of NaOH, KOH, or H_2SO_4 over a week, showing strong resistance to attack by acids and bases. However, Lu et al. modified the surface chemistry of

☆ This paper presented at the 2nd National Congress on Fuel Cells, Conappice 2006.

* Corresponding author. Tel.: +34 976 733977; fax: +34 973 733318.
E-mail address: mlazaro@icb.csic.es (M.J. Lázaro).

0378-7753/$ – see front matter © 2007 Elsevier B.V. All rights reserved.
doi:10.1016/j.jpowsour.2007.01.042

CMK-5 carbon using the mild oxidizing agent H_2O_2 in order to introduce oxygen surface groups while its ordered structure was maintained, but surprisingly a structural collapse occurred [30].

The objectives of this study are to modify ordered mesoporous carbons by chemical treatment maintaining their ordered structure and to determine their effect on the dispersion and catalytic performance of platinum electrocatalysts supported on functionalized OMC. In this work, ordered mesoporous carbons were synthesised using SBA-15 silica as template. Their texture and surface chemistry were modified by oxidation treatments in liquid phase using nitric acid at different concentrations as oxidative agent. Ordered mesoporous carbons were used as platinum catalyst supports using the method of reduction with $NaBH_4$. OMC were characterized by means of N_2-physisorption, X-ray diffraction (XRD), transmission electronic microscopy (TEM) and temperature programmed desorption (TPD). Methanol and carbon monoxide oxidation at platinum supported electrocatalysts were studied electrochemically by cyclic voltammetry. Current–time curves were recorded in order to establish the activity towards these reactions.

2. Experimental

2.1. Synthesis of SBA-15 and ordered mesoporous carbon

Mesoporous silica SBA-15 was prepared from a triblock $EO_{20}PO_{70}EO_{20}$ copolymer (Aldrich) and TEOS (Aldrich) as silica source, as described elsewhere [31]. In a typical synthesis, 10 g of triblock copolymer was added to 300 ml of an aqueous solution of 1.7 M hydrochloric acid and stirred at 50 °C for 2 h. Next, 20 g of TEOS was added dropwise and the mixture was stirred at the same temperature for 2 h. The synthesised gels were kept at 108 °C for 24 h under static conditions. The final products were filtered, washed with distilled water and dried firstly at room temperature for 24 h and secondly at 108 °C for 24 h. The synthesised samples were calcined under N_2 atmosphere at 500 °C.

Ordered mesoporous carbons were prepared by incipient wetness impregnation at room temperature of SBA-15 with a mixture of furan resin (Huttenes Albertus) and acetone (mass ratio resin:acetone = 5:1), and nitric acid was used as catalyst. Then, impregnated SBA-15 sample was cured at 108 °C for 1 day and carbonised at 700 °C for 3 h. A silica–carbon composite was obtained. Finally, samples were washed with HF to remove SBA-15 and washed with distilled water. After that, carbon support (CMK3) was dried at 108 °C for 24 h.

2.2. Functionalization of carbon supports

The texture and surface chemistry of synthesised mesoporous carbon were modified by means of different oxidation treatments in liquid phase to optimise their ability of dispersing active metal particles. Mesoporous carbon was refluxed in HNO_3 2 M (CMK3-Nd) or concentrated HNO_3 (CMK3-Nc) at room temperature for 0.5 or 2 h in order to create oxygen surface groups. Finally, carbon supports were filtered, washed with distilled water and dried at 108 °C for 12 h.

2.3. Preparation of platinum electrocatalysts

Platinum supported electrocatalysts were prepared by reduction of H_2PtCl_6 with sodium borohydride [32]. Appropriate concentrations were used to obtained a platinum loading of 20 wt.% metal on the different mesoporous carbon materials (including the untreated CMK3). For the sake of comparison, the same procedure was employed with Vulcan XC-72 (Cabot) as support.

2.4. Physical and structural characterization

Textural and surface chemistry properties of carbon supports were characterized by N_2-physisorption and temperature programmed desorption, respectively. For the structural characterization, transmission electronic microscopy and X-ray diffraction were used.

Nitrogen adsorption–desorption isotherms were measured at 77 K using a Micromeritics ASAP 2020. Total surface area and pore volumes were determined using the Brunauer–Emmett–Teller (BET) equation and the single point method, respectively. Pore size distribution (PSD) curves were calculated by Barrett–Joyner–Halenda (BJH) method. The position of the maximum of the PSD was used as the average pore diameter.

X-ray diffraction patterns at small angles ($2\theta = 0.5$–5°) were recorded using a Bruker AXS D8 Advance diffractometer with a θ–θ configuration and using Cu Kα radiation.

TEM images for determination of particle size and morphology as well as metal dispersion of samples were obtained using a 300 kV Philips CM-30 TEM. For such measurements, the samples were suspended in ethanol with ultrasonic dispersion for 3 min. Then a drop of this suspension was deposited on a holey carbon grid and, after drying, the grid was ready for observation. TEM images of the samples were recorded both in the axial direction of the ordered hexagonal pores and in the perpendicular direction. Accurate orientation control by means of specimen tilting was sometimes necessary for obtaining images with clearly resolved pore contours. Images were recorded with a MultiScan CCD camera (model 794, Gatan) using low-dose conditions. Fourier transform from images was performed using Digital Micrograph software (Version 3.7.0, Gatan).

The determination of the amount of oxygen surface groups of the supports was carried out by means of temperature programmed desorption experiments. Typically, 300 mg were placed in a U-shaped quartz reactor. The temperature was increased at a rate of 10 °C min^{-1} up to 1050 °C under a helium flow of 30 ml min^{-1}. The amounts of CO and CO_2 desorbed from the carbon samples were analysed by gas chromatography.

2.5. Electrochemical studies

Electrochemical studies were carried out using an AUTOLAB PGSTAT302. All experiments were carried out in electrochemical flow cells using a three-electrode assembly at room temperature. A high surface area carbon rod was used as counter electrode and a reversible hydrogen electrode (RHE) in

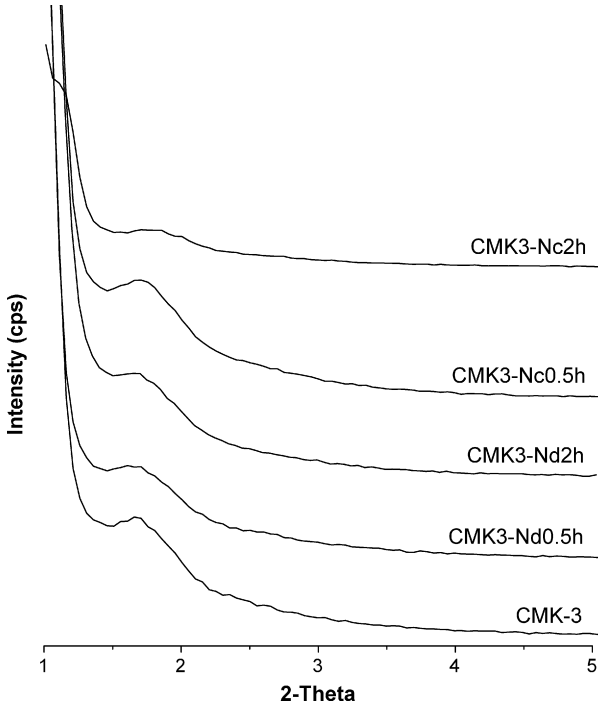

Fig. 1. XRD patterns of CMK3 carbons.

Table 1
Amounts of CO and CO_2 desorbed during TPD experiments

Sample	CO (mmol g^{-1})	CO_2 (mmol g^{-1})	$CO + CO_2$ (mmol g^{-1})	CO/CO_2
CMK3	1.77	0.74	2.51	2.4
CMK3-Nd0.5h	2.42	0.60	3.02	4
CMK3-Nd2h	2.97	1.11	4.08	2.7
CMK3-Nc0.5h	3.57	1.88	5.45	1.9
CMK3-Nc2h	3.60	2.05	5.65	1.8

the supporting electrolyte was employed as reference electrode. All potentials in the text are referenced to this electrode. These experiments were carried out in 0.5 M H_2SO_4 at 30 °C, prepared from high purity reagents (Merck p.a.) and Milli-Q water (Millipore). The electrolyte was saturated with pure argon (99.998%, Air Liquide) or CO gases (99.997%, Air Liquide), depending on the experiments.

To characterize the quality of the electrocatalysts, cyclic voltammograms (CVs) were recorded in the supporting electrolyte solution between 0.05 and 1.10 V at a scan rate of 0.05 V s^{-1} in 0.5 M (base electrolyte). Electrochemical active areas were determined from the integration of the hydrogen region assuming 210 μC cm^{-2} involved in the desorption of a H_{ad} monolayer.

CO stripping voltammograms were obtained after bubbling this gas in the cell for 10 min at 0.20 V, followed by electrolyte exchange and argon purging to remove the excess of CO. The admission potential was selected considering that for this value maximum adsorbate coverage is achieved for CO adsorption on Pt. CVs were obtained in the 0.05–1.10 V potential range, starting from 0.20 V at a scan rate of 0.02 V s^{-1}.

Current–time curves were recorded at 0.70 V in a 0.5 M methanol + 0.5 M H_2SO_4 solution in order to evaluate the performance of the catalysts for the oxidation of this compound.

3. Results and discussion

3.1. Characterization of carbon supports

Fig. 1 shows the small-angle XRD patterns of CMK3 carbons before and after oxidation treatments. CMK3 carbon shows one peak at small angles indicating that the sample presents an ordered porous structure. This peak is characteristic of hexagonal symmetries. Oxidized samples show similar XRD patterns indicating that hexagonally ordered structure is maintained after oxidation treatments. However, CMK3 treated with concentrated HNO_3 for 2 h shows a smaller peak suggesting a decrease of the structural order, although it still has a considerable degree of structural order.

TEM images showed in Fig. 2A and B confirm that the structure of CMK3 is highly ordered. The images were recorded along two different crystallographic directions which show the typical features of CMK3. The structure is an inverse replica of the structure of SBA-15 silica used as template. After oxidation treatments, ordered structure is maintained, as it can be seen in Fig. 2C–F. Fig. 2F shows that carbon treated with concentrated HNO_3 for 2 h, that is the most severe treatment, maintains the ordered structure although its degree of structural order is lower than the rest of the samples, as observed by XRD.

Temperature programmed desorption experiments give information about the surface oxygen groups that are created on CMK3 carbons during the oxidation treatments. Table 1 shows the amounts of CO and CO_2, desorbed during TPD experiments, and the ratio CO/CO_2. Results demonstrate that an increase in severity of the oxidation treatments results in an increase in the number of oxygen surface groups. On the other hand, the ratio CO/CO_2, which can be taken as a measure of the surface acidity, decreases with the severity of the treatments

Table 2
Textural parameters of the CMK-3 carbons

Sample	S_{BET} (m^2 g^{-1})	V_{TOTAL} (cm^3 g^{-1})	V_{MICRO} (cm^3 g^{-1})	V_{MESO} (cm^3 g^{-1})	S_{MICRO} (m^2 g^{-1})	S_{MESO} (m^2 g^{-1})
CMK-3	577	0.37	0.07	0.30	133	444
CMK3-Nd0.5h	532	0.34	0.07	0.27	126	406
CMK3-Nd2h	436	0.29	0.04	0.25	80	336
CMK3-Nc0.5h	406	0.27	0.04	0.23	78	330
CMK3-Nc2h	401	0.26	0.04	0.22	71	328

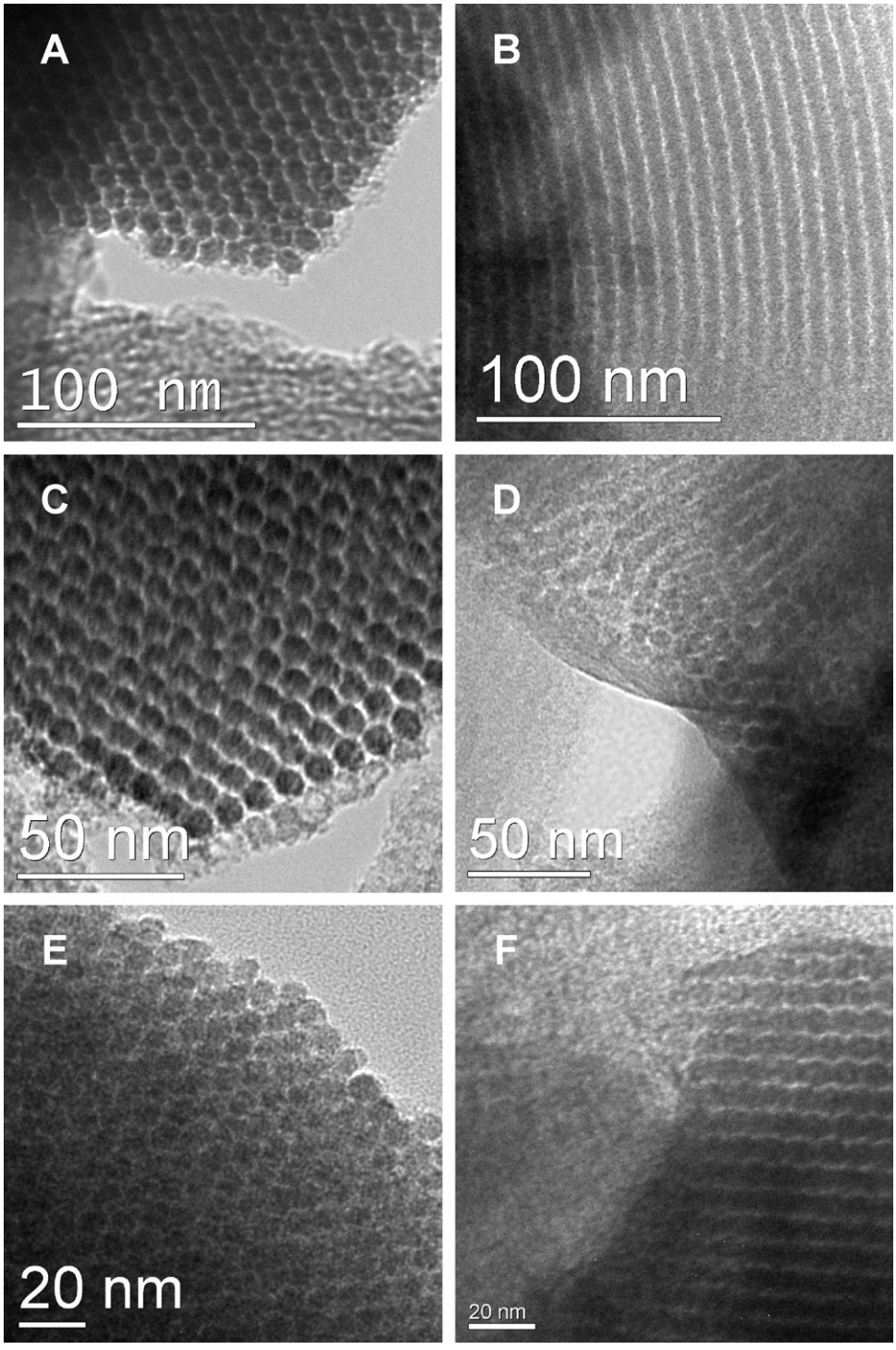

Fig. 2. TEM images of CMK3 carbons. (A) Hexagonal structure of CMK3 carbon, (B) parallel mesopores of CMK3 carbon, (C) CMK3-Nd0.5h, (D) CMK3-Nd2h, (E) CMK3-Nc0.5h and (F) CMK3-Nc2h.

indicating that the number of acidic surface sites increases [33]. Acidic sites are mainly attributed to carboxylic acid functions which are expected to have the major influence in the platinum dispersion [26]. It is observed that samples treated with concentrated HNO_3 have the greatest number of oxygen surface groups. However, CMK3 carbon treated with HNO_3 for 2 h has a lower structural order, as observed by TEM and XRD.

In order to further investigate how the pore structure and textural properties of the CMK3 carbon were changed during the oxidation treatments, CMK3 carbons were characterized by means of N_2-physisorption. Table 2 contains the textural properties of the carbon samples before and after oxidation treatments. All samples exhibit high surface areas and large pore volumes, as can be seen in Table 2. The surface area and pore volume of

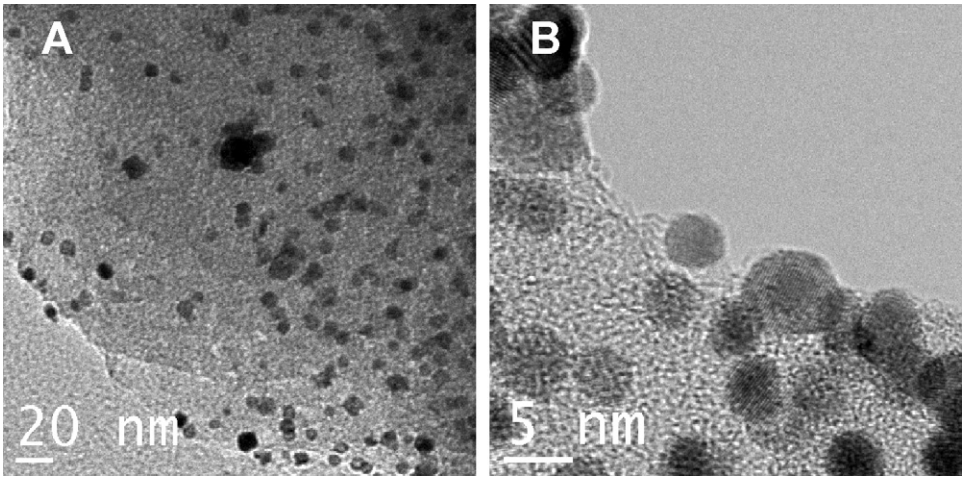

Fig. 3. TEM images of platinum supported on CMK3-Nc0.5h.

CMK3 decrease after oxidation treatments indicating that the ordered structure has been lightly affected. However, HNO_3 treatments do not change the average pore diameter, that is 2.5 nm, and no micropores are formed.

3.2. Electrochemical characterization: the effect of the support treatment

Pt supported electrocatalysts are well dispersed on the carbon support as it can be seen, for example, in Fig. 3 for Pt/CMK3-Nc0.5h, leading to nanoparticles in the 3–5 nm range. It is remarkable that the crystalline structure of the metal is clearly visible in the nanoparticles (Fig. 3B).

Fig. 4 shows the CVs for the six materials studied during the stripping of a monolayer CO formed at 0.20 V, as well as the second cycle after oxidation which corresponds to the voltammogram in the base electrolyte for the clean surface. It is observed that the peak potential for the oxidation of CO is attained at 0.80 V with a shoulder at 0.71 V when Vulcan XC-72 is used. This is the common behaviour described in the literature for this material (for example, see Ref. [34]). For the case on untreated CMK3, only a very small contribution is apparent during the stripping, but it is shown in the second CV corresponding to the base electrolyte that, as expected, the amount of platinum is very small for this catalyst. Then, it is concluded that the functionalization is needed in order to support the metal.

For the electrocatalysts prepared with CMK3 treated with HNO_3, the oxidation of CO_{ad} occurs in all cases at more negative potentials with respect to that for Vulcan XC-72. This implies that CO can be easily oxidized at these materials. However, differences in the shape of the CVs are relevant. For CMK3 treated with concentrated HNO_3, a sharp peak located at around 0.70 V is developed, that is, a 0.10 V shift to more negative values is established. When CMK3 functionalized with 2 M HNO_3 is employed, two features are visible in the CVs. One is located near to the contribution at Vulcan XC-72, but the most important fact is the presence of the oxidation current at very low potentials (centred at 0.56 V). From these results, there is a good perspective for the application of these electrocatalysts for PEM fuel cells.

With the purpose to check the performance of these materials towards methanol electrooxidation, current–time curves were recorded at 0.70 V in a 0.5 M methanol solution in the base electrolyte (Fig. 5). It is shown that the highest stationary current density corresponds to the CMK3 carbon oxidized with 2 M HNO_3 during 0.5 h, and it is very low for both untreated CMK3 and that treated with the most extreme conditions (concentrated HNO_3 during 2 h). The other three electrocatalysts (Pt supported on Vulcan XC-72, CMK3 carbon prepared with 2 M

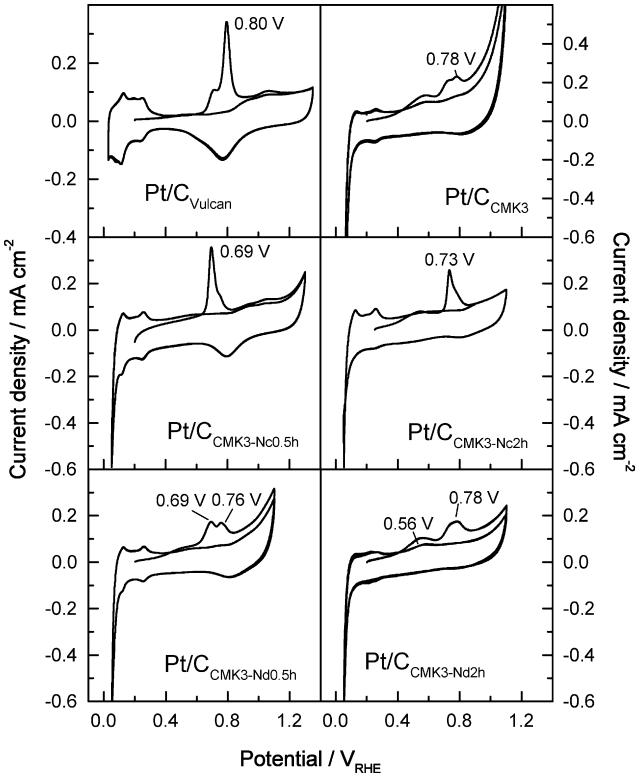

Fig. 4. CVs for the CO stripping in 0.5 M H_2SO_4 after adsorption at 0.20 V; $v = 20\,mV\,s^{-1}$.

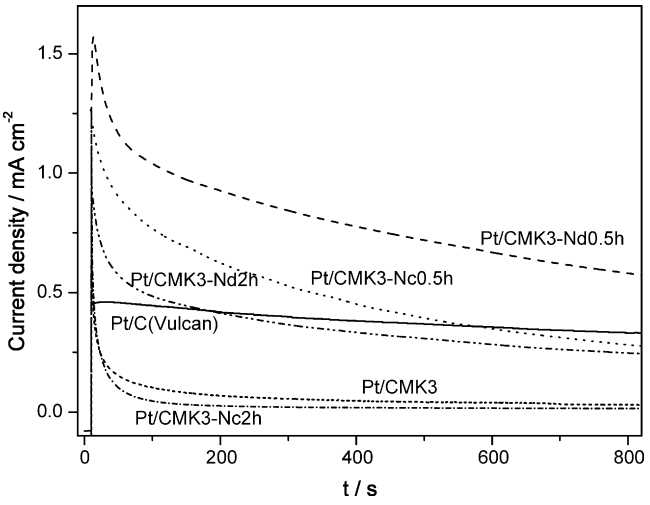

Fig. 5. Current density–time curves recorded in a 0.5 M methanol + 0.5 M H_2SO_4 solution at $E = 0.70$ V.

HNO_3 during 2 h and concentrated HNO_3 during 0.5 h) attain similar stationary currents. These data provide evidence of the need of a compromise between the concentration of the acid and the duration of the treatment.

4. Conclusions

Platinum electrocatalysts prepared on ordered mesoporous carbon have shown a good performance for methanol electrooxidation. OMC needs functionalization for anchoring the metal nanoparticles and this was performed with nitric acid as oxidative agent. During this process, it has been proved that oxygen surface groups were created and texture and surface chemistry altered, whereas the ordered porous structure was maintained. However, electrochemical studies show that treatment conditions influence the final currents achieved in a methanol solution, being the best the catalyst obtained from CMK3 oxidized with 2 M HNO_3 during 0.5 h.

The reasons for this behaviour are not clear. However, these are very promising results which represent a first step in the preparation and characterization of metal supported on OMC. Further studies on the physical properties of metal supported electrocatalysts are needed to understand the final performance of these materials and are at the moment in progress. Also bimetallic catalysts will be prepared, as it is well known that they produce an increase in efficiency of PEM fuel cells.

Acknowledgments

The authors gratefully acknowledge financial support given by the Spanish MEC under the projects NAN2004-09333-C05-03, MAT2005-06699-C03-01 and MAT2005-06699-C03-02 (Feder). EGB and LC acknowledge the Spanish government for their "Ramón y Cajal" contract and FPI grant, respectively. The authors are also indebted to the SCT-UB technical services for the TEM facilities.

References

[1] J.H. Tian, F.B. Wang, Z.H.Q. Shan, R.J. Wang, J.Y. Zhan, J. Appl. Electrochem. 34 (2004) 461–467.
[2] Z. Zhou, S. Wang, W. Zhou, L. Jiang, G. Wang, G. Sun, B. Zhou, Q. Xin, Phys. Chem. Chem. Phys. 5 (2003) 5485–5488.
[3] H. Kim, J.-N. Park, W.-H. Lee, Catal. Today 87 (2003) 237–245.
[4] J. Prabhuram, T.S. Zhao, C.W. Wong, J.W. Guo, J. Power Sources 134 (2004) 1–6.
[5] W.H. Lizcano-Valvuena, V.A. Paganin, C.A.P. Leite, F. Galembeck, E.R. Gonzalez, Electrochim. Acta 48 (2003) 3869–3878.
[6] M.J. Escudero, E. Hontañón, S. Schwartz, M. Boutomet, L. Daza, J. Power Sources 106 (2002) 206–214.
[7] Z.R. Ismagilov, M.A. Kerzhentsev, N.V. Shikina, A.S. Lisitsyn, L.B. Okhlopkova, Ch.N. Barnakov, M. Sakashita, T. Iijima, K. Tadokoro, Catal. Today 102–103 (2005) 58–66.
[8] L. Zhang, B. Cheng, E.T. Samulski, Chem. Phys. Lett. 398 (2004) 505–510.
[9] M. Gangeri, G. Centi, A. La Malfa, S. Perathoner, R. Vieira, C. Phram-Huu, M.J. Ledoux, Catal. Today 102–103 (2005) 50–57.
[10] F. Yuan, H.K. Yu, H. Ryu, Electrochim. Acta 50 (2004) 685–691.
[11] N. Rajalakshmi, H. Ryu, M.M. Shujumon, S. Ramaprabhu, J. Power Sources 140 (2005) 250–257.
[12] W. Li, C. Liang, J. Qiu, W. Zhou, H. Han, Z. Wei, G. Sun, Q. Xin, Carbon 40 (2002) 787–803.
[13] H. Tang, J.H. Chen, Z.P. Huang, D.Z. Wang, Z.F. Ren, L.H. Nie, Y.F. Luang, S.Z. Yao, Carbon 42 (2004) 191–197.
[14] P. Kim, H. Kim, J.B. Joo, W. Kim, I.K. Song, J. Yi, J. Power Sources 145 (2005) 139–146.
[15] A. Smirnova, X. Dong, H. Hara, A. Vasiliev, N. Sammes, Int. J. Hydrogen Energy 30 (2005) 149–158.
[16] J. Marie, S. Bretón-Fabry, P. Achard, M. Chatenet, A. Pradourat, E. Chainet, J. Non-Cryst. Solids 350 (2004) 88–96.
[17] P.V. Samant, C.M. Rangel, M.H. Romero, J.B. Fernandes, J.L. Figueiredo, J. Power Sources 151 (2005) 79–84.
[18] J.-H. Nam, Y.-Y. Jang, Y.-U. Kwon, J.-D. Nam, Electrochem. Commun. 6 (2004) 737–741.
[19] J. Ding, K.-Y. Chan, J. Ren, F.-S. Xiao, Electrochem. Commun. 50 (2005) 3131–3141.
[20] J.B. Joo, P. Kim, W. Kim, J. Kim, J. Yi, Catal. Today 111 (2006) 171–175.
[21] S.H. Joo, S.J. Choi, I. Oh, J. Kwak, Z. Liu, O. Terasaki, R. Ryoo, Nature 412 (2001) 169–172.
[22] R. Ryoo, S.H. Joo, M. Kruk, M. Jaroniec, Adv. Mater. 13 (2001) 677–681.
[23] A.B. Fuertes, D.M. Nevskaia, Microporous Mesoporous Mater. 62 (2003) 177–190.
[24] J. Kim, J. Lee, T. Hyeon, Carbon 42 (2004) 2711–2719.
[25] A.E. Aksoylu, M. Madalena, A. Freitas, M.F.R. Pereira, J.L. Figueiredo, Carbon 39 (2001) 175–185.
[26] C. Prado-Burguete, A. Linares-Solano, F. Rodríguez-Reinoso, J. Catal. 115 (1989) 98–106.
[27] M.A. Fraga, E. Jordão, M.J. Mendes, M.M.A. Freitas, J.L. Faria, J.L. Figueiredo, J. Catal. 209 (2002) 355–364.
[28] A. Sepúlveda-Escribano, F. Coloma, F. Rodríguez-Reinoso, Appl. Catal. A: Gen. 173 (1998) 247–257.
[29] R. Ryoo, S.H. Joo, S. Jun, T. Tsubakiyama, O. Terasaki, Stud. Surf. Sci. Catal. 135 (2001) 1121–1128.
[30] A.-H. Lu, W.-C. Li, N. Muratova, B. Spliethoff, F. Schüth, Chem. Commun. (2005) 5184–5186.
[31] P.F. Fulvio, S. Pikus, M. Jaroniec, J. Colloid Interface Sci. 287 (2005) 717–720.
[32] J.R.C. Salgado, E. Antolini, E.R. Gonzalez, J. Phys. Chem. B 108 (2004) 17767.
[33] J.L. Figueiredo, M.F.R. Pereira, M.M.A. Freitas, J.J.M. Órfão, Carbon 37 (1999) 1379–1389.
[34] G. García, J.A. Silva-Chong, O. Guillén-Villafuerte, J.L. Rodríguez, E.R. González, E. Pastor, Catal. Today 116 (2006) 415–421.